Antioxidant and cytoprotective effects of *Stachys riederi* var. *japonica* ethanol extract on UVA-irradiated human dermal fibroblasts

JI YEON HWANG[1], ANIL KUMAR YADAV[2], BYEONG-CHURL JANG[2] and YOUNG CHUL KIM[3]

[1]Department of Research and Development, Research Center for Natural Ingredients and New Materials, Daepyung Co., Ltd., Sangju 37112; [2]Department of Molecular Medicine, College of Medicine; [3]Department of Public Health, Faculty of Food and Health Sciences, Keimyung University, Daegu 42601, Republic of Korea

Received August 12, 2018; Accepted November 26, 2018

DOI: 10.3892/ijmm.2019.4048

Abstract. *Stachys riederi* is one of the largest genera in the flowering plant family Lamiaceae. The aqueous extract of *Stachys riederi* var. *japonica* is known for its anti-allergic effect. In the present study, the antioxidant and cytoprotective effects of *Stachys riederi* var. *japonica* ethanol extract (SREE) on ultraviolet A (UVA)-irradiated human dermal fibroblasts (HDFs) were evaluated. At 100 μg/ml, SREE significantly inhibited production of reactive oxygen species (ROS) in UVA-irradiated HDFs. SREE at 100 μg/ml additionally markedly interfered with the loss of mitochondrial membrane potential ($\Delta\Psi$m) in these cells. In addition, SREE at 100 μg/ml attenuated UVA-induced DNA fragmentation and caspase-3 activation in HDFs. SREE at 100 μg/ml additionally increased mRNA and protein expressions of Bcl-2 and decreased those of Bax and cytochrome *c* in UVA-irradiated HDFs. In summary, to the best of our knowledge, these results demonstrate for the first time that SREE exhibited antioxidant and cytoprotective effects on UVA-irradiated HDFs, which may be mediated through suppression of ROS generation, inhibition of the loss of $\Delta\Psi$m and inhibition of apoptosis.

Introduction

Solar ultraviolet (UV) radiation is the primary source of environmental damage for human skin. UV radiation is divided into two spectral regions: UVA (320-400 nm) and UVB (290-320 nm) constituting 96 and 4%, respectively, and each are responsible for UV overexposure-associated skin pathologies, including premature skin aging and skin cancer (1). Accordingly, UVA, which penetrates the dermal layers of skin more deeply compared with UVB, serves a principal role in these skin pathologies by generating reactive oxygen species (ROS) in the resident dermal fibroblasts and extracellular structures (2). A growing body of evidence additionally indicates that the overexposure of skin cells to UV rays triggers various cellular alterations, including cell cycle arrest, cell membrane disruption and nuclear DNA damage, leading to skin cell loss and/or apoptosis (3-6). Therefore, there is an urgent requirement to identify novel substances that may be potential skin-improving and cosmeceutical materials against UV insult, and may inhibit or lessen the cellular alterations triggered by UV overexposure.

Apoptosis is the process of programmed cell death, which involves a series of morphological and biochemical alterations, including cell detachment, cell shrinkage and nuclear DNA fragmentation (7,8). This process is regulated by the action of a variety of proteins and/or factors. For example, activation of the caspase family members, including caspase-9, caspase-8, and caspase-3, is crucial for apoptosis induction in UV-irradiated dermal fibroblasts or keratinocytes (9-11). In addition, members of the B-cell lymphoma-2 (Bcl-2) family, including Bcl-2 and Bcl-2-associated X protein (Bax), are involved in UV-induced apoptosis of dermal fibroblasts or keratinocytes (10,12). It is known that Bcl-2, as an anti-apoptotic protein, and Bax, as a pro-apoptotic protein, have important roles in competitively regulating the mitochondrial membrane integrity and the mitochondria-initiated caspase activation pathway (13). In addition, previous studies have demonstrated that a decrease or loss of the mitochondrial membrane potential ($\Delta\Psi$m) is an early event of apoptosis and cytochrome *c* release from the mitochondria to the cytosol additionally contributes to apoptosis induction by activating members of the caspase family, which cleaves critical proteins for cell survival and growth (14,15).

The genus *Stachys* is comprised of ~300 species worldwide, representing one of the largest genera of the Lamiaceae. Importantly, a number of *Stachys* species have been exploited

Correspondence to: Professor Byeong-Churl Jang, Department of Molecular Medicine, College of Medicine, Keimyung University, 1095 Dalgubeol-Daero, Daegu 42601, Republic of Korea
E-mail: jangbc123@gw.kmu.ac.kr

Professor Young Chul Kim, Department of Public Health, Faculty of Food and Health Sciences, Keimyung University, 1095 Dalgubeol-Daero, Daegu 42601, Republic of Korea
E-mail: yckim@kmu.ac.kr

Key words: *Stachys riederi* var. *japonica*, ultraviolet A, reactive oxygen species, caspase-3, apoptosis, human dermal fibroblasts

in traditional medicine as astringent, wound-healing, anti-diarrheal, anti-nephritic and anti-inflammatory agents (16-18). Notably, there is additionally evidence demonstrating an anti-allergic effect of the aqueous extract of *Stachys riederi* var. *japonica* (19). However, at present, the antioxidant and cytoprotective effects of *Stachys riederi* var. *japonica* on dermal cells remain unclear.

In the present study, the antioxidant and cytoprotective effects of *Stachys riederi* var. *japonica* ethanol extract (SREE) on UVA-irradiated human dermal fibroblasts (HDFs) were investigated. To the best of our knowledge, this is the first study to suggest that SREE has antioxidant and cytoprotective effects on UVA-irradiated HDFs, which may be mediated through regulation of ROS production, the $\Delta\Psi m$, expression of Bcl-2 and Bax, caspase-3 activity and apoptosis.

Materials and methods

Materials and apparatus. Dimethyl sulfoxide (DMSO; cat. no. D8418), ascorbic acid (AA; cat. no. A5960) and MTT (cat. no. M2128) were purchased from Sigma-Aldrich; Merck KGaA (Darmstadt, Germany). Dulbecco's modified Eagle's medium (DMEM; cat. no. BE12-604F) and penicillin/streptomycin (P/S) cocktail (cat. no. BW17-718R) were purchased from Lonza Group Ltd., (Basel, Switzerland). Fetal bovine serum (FBS; cat. no. S001-01) was purchased from WELGENE, Inc., (Gyeongsan, Republic of Korea). The anti-Bcl-2 (cat. no. ab7973) and anti-Bax (cat. no. ab7977) primary antibodies were obtained from Abcam (Cambridge, MA, USA). The anti-β-actin (cat. no. sc-81178) primary antibody was obtained from Santa Cruz Biotechnology, Inc. (Dallas, TX, USA). Horseradish peroxidase (HRP)-conjugated goat anti-rabbit immunoglobulin G (IgG; H+L; cat. no. 111-035-045) and goat anti-mouse IgG (H+L; cat. no. 115-035-062) secondary antibodies were purchased from Jackson ImmunoResearch Laboratories, Inc. (West Grove, PA, USA). UV irradiation was performed with a UVA sunlamp (Sankyo Denki, Hiratsuka, Japan). An inverted microscope (CKX41; Olympus Corporation, Tokyo, Japan) was used for observation of cell growth and a CO_2 incubator (MCO-17AC; Sanyo Electric Co., Ltd., Osaka, Japan) was used for cell culture. A rotary vacuum concentrator (BÜCHI R-205; BÜCHI Labortechnik AG, Flawil, Switzerland) was used for sample extraction.

Preparation of SREE. The root of *Stachys riederi* var. *japonica* was purchased from DONG UI Chosukjam Farmers, Inc. (Sancheong, Korea). A voucher specimen was deposited in the herbarium of our laboratory at the Department of Public Health, Faculty of Food and Health Sciences (Keimyung University, Daegu, Korea) with the plant identification no. KMU/J/638. A pulverized sample (50 g) was put into a flask and extracted in 500 ml 80% ethanol three times for 24 h each at 25˚C. The extract was filtered and concentrated using rotary vacuum evaporator followed by lyophilization (yield 46.7%).

Cell culture. HDFs (Amore Pacific Company, Seoul, Korea) were grown in DMEM supplemented with 10% heat-inactivated FBS and 1% P/S cocktail in a humidified atmosphere of 95% air and 5% CO_2 at 37˚C.

Measurement of cell viability. The effect of SREE on the viability of HDFs was assessed by MTT assay. HDFs were seeded in a 96-well plate ($1x10^4$ cells/100 μl/well) overnight. HDFs were treated with different concentrations of SREE (25, 50, 100 and 200 μg/ml) for 48 h. Subsequently, MTT (0.5 mg/ml) was added to each well of the 96-well plate and the cells were incubated at 37˚C for an additional 3 h. The 96-well plate was centrifuged 25˚C at 168 x g for 10 min. Following removal of the supernatant, 200 μl DMSO was added to each well. Subsequent to dissolving the formazan with DSMO in the cells with a plate-shaker for 15 min, the absorbance at 540 nm was read using an ELISA plate reader.

UVA irradiation. HDFs were cultivated in a culture dish ($1.5x10^5$ cells/ml) until they reached ~80% confluence. Following removal of the culture medium, HDFs were washed with PBS and exposed to 6.3 J/cm^2 UVA in DMEM without FBS prior to treatment with SREE or AA.

Measurement of cellular ROS levels. Cellular ROS levels were measured using dichloro-dihydro-fluorescein-diacetate (DCFH-DA). Following UVA irradiation, HDFs were incubated at 37˚C with freshly prepared pre-warmed 10 mM DCFH-DA for 20 min. HDFs were subsequently rinsed twice with PBS and levels of green fluorescence, corresponding to the levels of cellular ROS, were detected through a 520 nm long-pass filter on an FV-1000 laser fluorescence microscope (Olympus Corporation; magnification, x100). The levels of cellular ROS were quantified by a fluoro-photometer with DataMax version 2.2 and GRAMS/32 software (HORIBA Jobin Yvon, Inc., Edison, NJ, USA), using an excitation wavelength of 480 nm and an emission wavelength of 530 nm.

Semi quantitative reverse transcription-polymerase chain reaction (RT-PCR). Following treatment, total RNA from the conditioned HDFs was isolated using TRIzol® (Thermo Fisher Scientific, Inc., Waltham, MA, USA) according to the manufacturer's protocol. Equal amounts of total RNA (5 μg) were reverse transcribed in a 40 μl reaction mixture containing 8 μl Molony Murine Leukemia Virus Reverse Transcriptase (M-MLV RT) 5X buffer, 3 μl 10 mM dNTPs, 0.45 μl 40 U/μl RNase inhibitor, 0.3 μl 200 U/μl M-MLV RT (Promega Corporation, Madison, WI, USA) and 3.75 μl 20 μM oligo dT (Bioneer Corporation, Daejeon, Korea). Single-stranded cDNA was amplified by PCR using 4 μl 5X Green Go-Taq® Flexi reaction buffer, 0.4 μM 10 mM dNTPs, 0.1 μl 5 U/μl Taq polymerase, 1.2 μl 25 mM $MgCl_2$ (Promega Corporation), and 0.4 μl primer (20 pM/μl). The primer sequences used for PCR were as follows: Bcl-2 forward, 5'-CGACGACTTCTC CCGCCGCTACCGC-3' and reverse, 5'-CCGCATGCTGGG CCGTACAGTTCC-3'; Bax forward, 5'GGCAATCTGACC TTCAACTG-3' and reverse, 5'-AGTCTCTTGAGGACCCA ACC-3'; β-actin forward, 5'-CCCACTAACATCAAATG GGG-3' and reverse, 5'-ACACATTGGGGGTAGGAACA-3'. The PCR thermocycler conditions were as follows: Bcl-2, 38 cycles of denaturation at 94˚C for 1 min, annealing at 56˚C for 90 sec and extension at 72˚C for 2 min; Bax, 35 cycles of

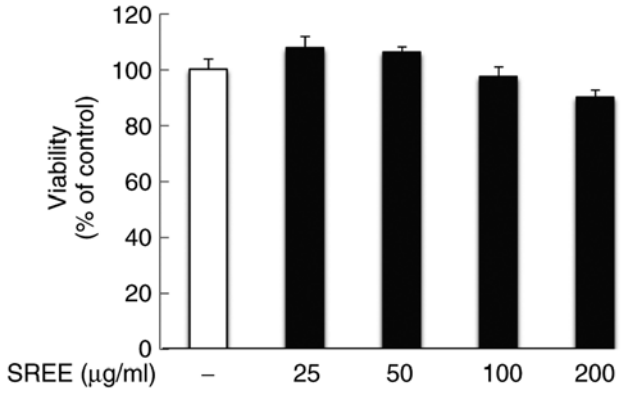

Figure 1. Effect of SREE on viability of HDFs. HDFs were treated without or with SREE or vehicle control (dimethyl sulfoxide) at the indicated concentrations (25, 50, 100 or 200 μg/ml) for 48 h, then subjected to the MTT assay. Values are presented as the mean ± standard deviation of three independent experiments. SREE, *Stachys riederi* var. *japonica* ethanol extract; HDFs, human dermal fibroblasts.

denaturation at 94˚C for 1 min, annealing at 58˚C for 1 min and extension at 72˚C for 2 min. The expression level of β-actin mRNA was used as an internal control to evaluate the relative mRNA expression of Bcl-2 and Bax. PCR products were visualized using ethidium bromide staining on a 1.2% agarose gel. DNA band density was semi-quantitatively analyzed using a Kodak Gel Logic 100 image analysis system with Kodak molecular imaging software, version 4.0 (Eastman Kodak Company, Rochester, NY, USA).

Preparation of whole cell lysates. Following treatment, HDFs were washed with PBS and lysed on ice for 15 min using 0.1 M Tris-HCl (pH 7.2) buffer containing 1% Nonidet P-40, 0.01% SDS and a protease inhibitor cocktail (Roche Diagnostics GmbH, Mannheim, Germany). Following centrifugation at 12,074 x g for 20 min at 4˚C, the supernatants were collected, and protein concentrations were determined by bicinchoninic acid assay (Pierce; Thermo Fisher Scientific, Inc.).

Western blot analysis. Equal amounts of protein (10 μg) were separated by 10% SDS-PAGE and transferred onto nitrocellulose membranes (EMD Millipore, Billerica, MA, USA). The membranes were washed with TBS (10 mM Tris-Cl, 150 mM NaCl; pH 7.5) with 0.05% (v/v) Tween-20 (TBST) followed by blocking for 2 h at 25˚C with TBST containing 5% (w/v) non-fat dried milk. The membranes were incubated overnight with antibodies specific for Bcl-2 (1:1,000), Bax (1:500) or β-actin (1:10,000) at 4˚C. The membranes were subsequently exposed to HRP-conjugated secondary antibodies of a goat anti-rabbit IgG (H+L; 1:2,000) or goat anti-mouse IgG (H+L; 1:2,000) for 2 h at room temperature and additionally washed three times with TBST. Immunoreactivity was detected using an enhanced chemiluminescence reagent according to the manufacturer's protocol (Amersham; GE Healthcare, Chicago, IL, USA). Band intensity was semi-quantified using ImageJ software (version 1.8.0; National Institutes of Health, Bethesda, MD, USA). β-actin was used as an internal control.

Measurement of the ΔΨm. The ΔΨm was visualized by using 5,5',6,6'-tetrachloro-1,1'3,3'-tetrathylbenzimidazolyl-carbocyanine iodide (JC-1) staining. JC-1 aggregates and monomers represent high and low ΔΨm, as indicated by red and green fluorescence, respectively. Following treatment, HDFs were incubated with 5 μg/ml JC-1 for 30 min at 37˚C. JC-1 monomers and JC-1 aggregates were observed at an emission wavelength of 488 nm (green) and 561 nm (red), respectively. Images were acquired using an FV-1000 laser fluorescence microscope (Olympus Corporation; magnification, x400).

Measurement of cellular caspase-3 activity. Following treatment, caspase-3 activity in HDFs was determined using a colorimetric caspase-3 assay kit (cat. no. APT165; EMD Millipore) according to the manufacturer's protocol. Following UVA irradiation, HDFs were harvested and lysed in cell lysis buffer (cat. no. 90065) provided in the assay kit. Assays were performed in 96-well microtiter plates by incubating 20 μg cell lysates in 100 μl reaction buffer (1% NP-40, 20 mM Tris-HCl, pH 7.5, 137 mM NaCl, 10% glycerol) containing a caspase substrate (Asp-Glu-Val-Aspchromophore-*p*-nitroanilide). Lysates were incubated at 37˚C for 90 min. Subsequently, the absorbance at 405 nm was measured with a spectrophotometer.

DNA fragmentation assay. Following treatment, HDFs were washed with PBS and lysed in a lysis buffer [0.3 M Tris-HCl (pH 7.5), 0.1 M NaCl, 0.01 M EDTA and 0.2 M sucrose] followed by the addition of RNase A (0.5 μg/ml) for an additional 18 h at 55˚C. The lysates were centrifuged at 25˚C, 10,000 x g for 20 min, and nuclear DNA in the supernatant was extracted with an equal volume of neutral phenol-chloroform-isoamyl alcohol mixture (25:24:1) and analyzed by electrophoresis on a 1.7% agarose gel. DNA was visualized and images were captured under UV illumination following staining with ethidium bromide (0.1 μg/ml). All observations made concerning this data were made visually.

Statistical analysis. Data are presented as the mean ± standard deviation of three independent experiments. Differences between groups were evaluated by one-way analysis of variance followed by a Duncan multiple range test for post-hoc comparison using SPSS 21.0 (IBM Corp., Armonk, NY, USA). $P<0.05$ was considered to indicate a statistically significant difference.

Results

SREE has no or low cytotoxic effects on HDFs. Initially, the effect of treatment with SREE at different concentrations for 48 h on the growth of HDFs was evaluated by an MTT assay. Notably, compared with the control (vehicle), treatment with SREE at 25 and 50 μg/ml slightly increased the viability of HDFs (Fig. 1). In addition, treatment with SREE at 100 and 200 μg/m only decreased the viability of HDFs by 2.7 and 9.9%, respectively. These results suggest that SREE at the concentrations examined has no or little cytotoxicity to HDFs.

SREE inhibits cellular ROS production in UVA-irradiated HDFs. To identify any antioxidant activity of SREE, the effect of treatment with SREE at different concentrations for 24 h on ROS production in UVA-irradiated HDFs was examined using fluorescence microscopy. For this, the fluorescein derivative

DCFH-DA, a redox indicator, was used. As demonstrated in Fig. 2A, compared with the control (no UVA), HDFs exposed to UVA exhibited extensive green fluorescence staining, indicative of a marked increase in cellular ROS generation following UVA exposure. However, treatment with SREE led to a concentration-dependent decrease in green fluorescence staining in UVA-irradiated HDFs. As hypothesized, 100 μg/ml treatment with AA, used as an antioxidant positive control, additionally markedly decreased UVA-induced green fluorescence staining in HDFs. The quantitative fluorescence intensity is presented in Fig. 2B. Compared with UVA-treated HDFs, treatment with SREE at 50, 100 and 200 μg/ml decreased ROS generation by 6.7, 24.0 and 30.1%, respectively. It was additionally observed that 100 μg/ml AA treatment decreased ROS generation, similar to the inhibition by SREE at 200 μg/ml.

SREE inhibits loss of the ΔΨm in UVA-irradiated HDFs. Given that disruption of the ΔΨm is crucial for UV-induced apoptosis of human keratinocytes (20), the present study aimed to examine whether UVA altered the ΔΨm in HDFs, and if SREE was involved, using fluorescence microscopy. The ΔΨm was visualized by JC-1 staining, in which high and low ΔΨm were indicated by JC-1 aggregates (red) and JC-1 monomers (green), respectively. As demonstrated in Fig. 3, control HDFs (no UVA) exhibited marked red staining. However, HDFs that were exposed to UVA exhibited extensive green staining, suggesting a decrease of the ΔΨm in UVA-irradiated cells. Notably, while treatment with SREE at 50 μg/ml had no effect on UVA-induced decrease of the ΔΨm in HDFs, SREE treatment at 100 or 200 μg/ml led to a concentration-dependent increase of red staining in the cells. At 100 μg/ml, AA treatment additionally markedly inhibited the UVA-induced decrease of the ΔΨm in HDFs.

SREE increases protein and mRNA expression levels of Bcl-2; however, decreases those of Bax in UVA-irradiated HDFs. The effect of SREE treatment at different concentrations for 24 h on the protein expression levels of Bcl-2 and Bax, mitochondrial membrane-associated proteins, was subsequently determined in UVA-irradiated HDFs using western blot analysis. As demonstrated in Fig. 4A, compared with the control (no UVA), UVA irradiation did not significantly affect the protein expression of Bcl-2 in HDFs. However, UVA irradiation markedly increased the protein expression of Bax in HDFs. Notably, SREE treatment concentration-dependently increased the protein expression of Bcl-2 in UVA-irradiated HDFs. In addition, SREE treatment concentration-dependently inhibited the ability of UVA to increase Bax protein expression in HDFs. At 100 μg/ml, treatment with AA additionally led to a slight increase in Bcl-2 protein expression and decreased expression levels of Bax protein in UVA-irradiated HDFs, compared with cells exposed to only UVA. RT-PCR assays were performed to examine whether SREE affected mRNA expression levels of Bcl-2 and Bax in UVA-irradiated HDFs. As presented in Fig. 4B, compared with the control (no UVA), UVA irradiation markedly downregulated mRNA expression of Bcl-2 while upregulated that of Bax in HDFs. Notably, SREE treatment at the concentrations examined markedly attenuated the ability of UVA to downregulate Bcl-2 mRNA expression in HDFs.

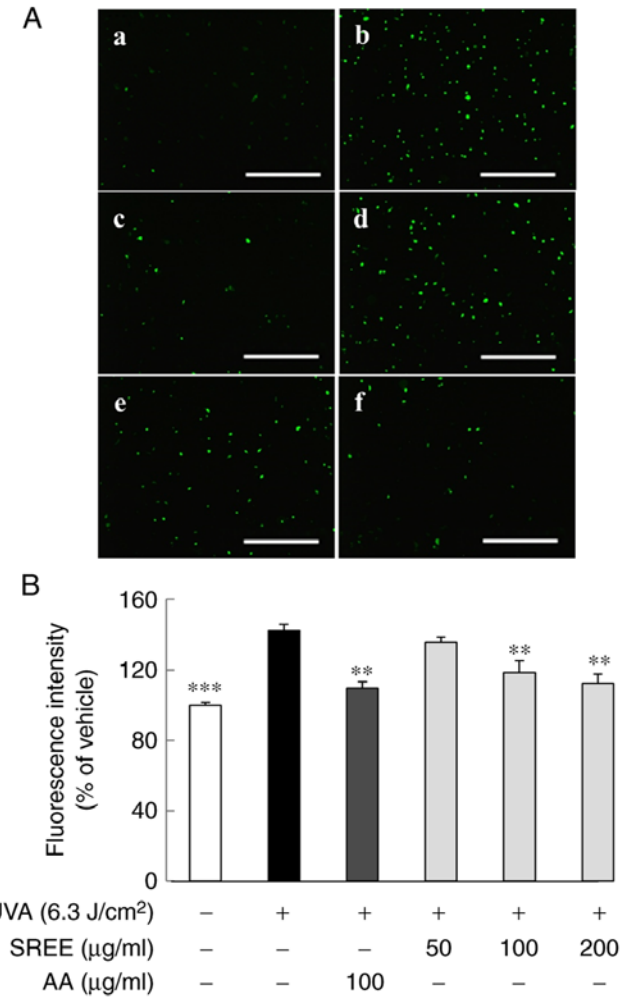

Figure 2. Effect of SREE on ROS generation in UVA-irradiated HDFs. (A) Fluorescence detection of cellular ROS levels in UVA-irradiated HDFs in the absence or presence of SREE or AA at the indicated concentrations for 24 h. (A-a) no SREE or AA. (A-b) 6.3 J/cm^2 UVA. (A-c) 6.3 J/cm^2 UVA plus 100 μg/ml AA. (A-d) 6.3 J/cm^2 UVA plus 50 μg/ml SREE. (A-e) 6.3 J/cm^2 UVA plus 100 μg/ml SREE. (A-f) 6.3 J/cm^2 UVA plus 200 μg/ml SREE. ROS generation was measured by dichloro-dihydro-fluorescein-diacetate fluorescence. Each picture is a representative fluorescent image of the conditioned cells visualized through a 520 nm long-pass filter on an Olympus FV-1000 laser fluorescence microscope. Magnification, x100 (scale bar, 150 μm). (B) Cellular ROS levels in HDFs were quantified by fluoro-photometer at an excitation wavelength of 480 nm and an emission wavelength of 530 nm. Values are presented as the mean ± standard deviation of three independent experiments. **P<0.01, ***P<0.001 vs. control (UVA only). SREE, *Stachys riederi* var. *japonica* ethanol extract; ROS, reactive oxygen species; UVA, ultraviolet A; HDFs, human dermal fibroblasts; AA, ascorbic acid.

In addition, SREE treatment concentration-dependently inhibited UVA-induced Bax mRNA upregulation in HDFs. Compared with the cells exposed to only UVA, AA treatment at 100 μg/ml additionally markedly inhibited the ability of UVA to decrease the mRNA expression of Bcl-2 and increase that of Bax in HDFs.

SREE inhibits the activation of caspase-3 in UVA-irradiated HDFs. The effects of SREE treatment at different concentrations for 24 h on the activity of caspase-3, a member of the caspase family involved in UV-induced apoptosis (20), was investigated in UVA-irradiated HDFs. As demonstrated in Fig. 5, compared with the control (no UVA), UVA irradiation

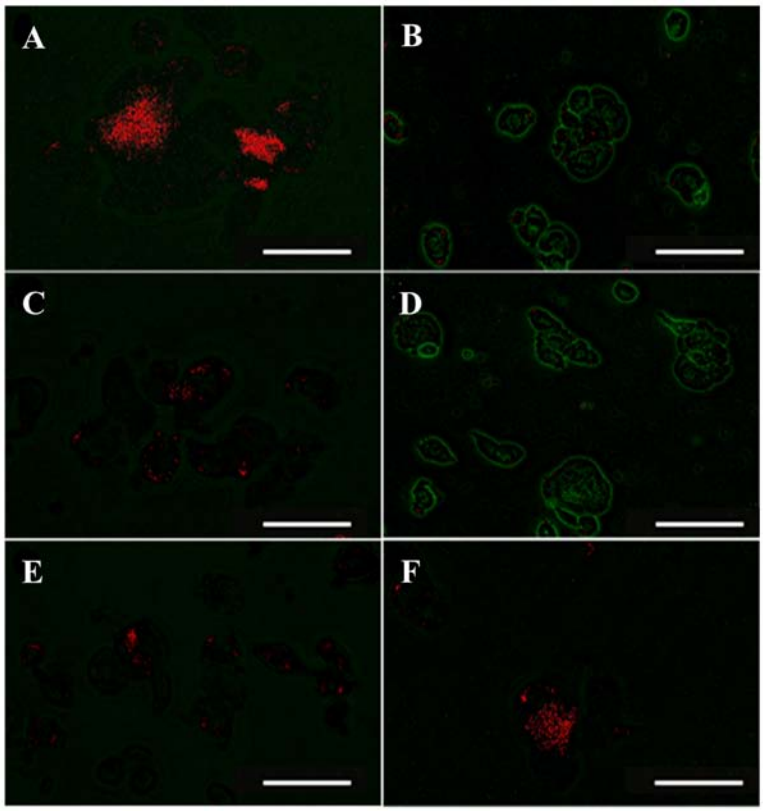

Figure 3. Effect of SREE on the mitochondrial membrane potential in UVA-irradiated HDFs. Fluorescence detection of the mitochondrial membrane potential in UVA-irradiated HDFs in the absence or presence of SREE or AA at the indicated concentrations for 24 h. (A) no SREE or AA with JC-1. (B) 6.3 J/cm^2 UVA with JC-1. (C) 6.3 J/cm^2 UVA plus 100 μg/ml AA with JC-1. (D) 6.3 J/cm^2 UVA plus 50 μg/ml SREE with JC-1. (E) 6.3 J/cm^2 UVA plus 100 μg/ml SREE with JC-1. (F) 6.3 J/cm^2 UVA plus 200 μg/ml SREE with JC-1. The mitochondrial membrane potential staining by JC-1 monomers and JC-1 aggregates is indicative of low (green) and high (red) mitochondrial membrane potential, respectively. Representative fluorescent images of the conditioned cells were detected with Olympus FV-1000 laser fluorescence microscope. Magnification, x400 (scale bar, 150 μm). SREE, *Stachys riederi* var. *japonica* ethanol extract; AA, ascorbic acid; UVA, ultraviolet A; HDFs, human dermal fibroblasts; JC-1, 5,5',6,6'-tetrachloro-1,1'3,3'-tetrathylbenzimidazolyl-carbocyanine iodide.

substantially increased the activity of caspase-3 in HDFs. SREE treatment at the concentrations examined significantly attenuated the ability of UVA to activate caspase-3 in HDFs. However, treatment with AA at 100 μg/ml did not significantly inhibit UVA activation of caspase-3 in HDFs.

SREE inhibits UVA-induced DNA fragmentation HDFs. Given that nuclear DNA fragmentation is a hallmark of apoptosis (7,21), whether UVA induces DNA fragmentation in HDFs, and whether SREE is involved in the mechanism, was examined using a DNA fragmentation assay. As indicated in Fig. 6, compared with the control (no UVA), UVA irradiation markedly induced DNA fragmentation in HDFs. Notably, SREE treatment inhibited UVA-induced DNA fragmentation in HDFs in a concentration-dependent manner. AA treatment at 100 mg/ml additionally markedly inhibited UVA-induced DNA fragmentation in HDFs.

Discussion

The aqueous extract of *Stachys riederi* var. *japonica* is known for its anti-allergic effects (19). To gain additional insight into the potential use of *Stachys riederi* as novel skin improving and/or cosmeceutical material, SREE was prepared and its antioxidant and cytoprotective effects on UVA-irradiated HDFs were investigated the present study. To the best of our knowledge, the present study demonstrated for the first time that SREE exhibited antioxidant and cytoprotective effects on UVA-irradiated HDFs through regulation of ROS production, the $\Delta\Psi$m, expression of Bcl-2 and Bax, caspase-3 activity and apoptosis.

It has been demonstrated that the exposure of UVA into skin cells rapidly and markedly increases the amounts of cellular ROS (2), suggesting UVA-induced oxidative stress. Excessive ROS causes cellular damage to a number of biological molecules including lipids, proteins and DNA (22). At present, the mechanism of SREE regulation of UVA-induced ROS production in dermal cells remains unclear. Notably, the results of the fluorescence microscopy in the present study demonstrated that SREE markedly decreased the cellular ROS levels in UVA-irradiated HDFs, suggesting the antioxidant effects of SREE.

It has been indicated that impairment of the mitochondrial function leads to cellular ROS generation in skin cells in response to UVA exposure (23). It has been established that mitochondrial membrane integrity is markedly affected by the expression levels of the Bcl-2 family proteins (24). For example, Bcl-2 is a mitochondrial membrane-associated protein that inhibits apoptosis (25,26). The anti-apoptotic role of Bcl-2 against cell death is supported by previous studies, which demonstrated that Bcl-2 overexpression abrogates UVB-induced apoptosis in human keratinocytes *in vitro*

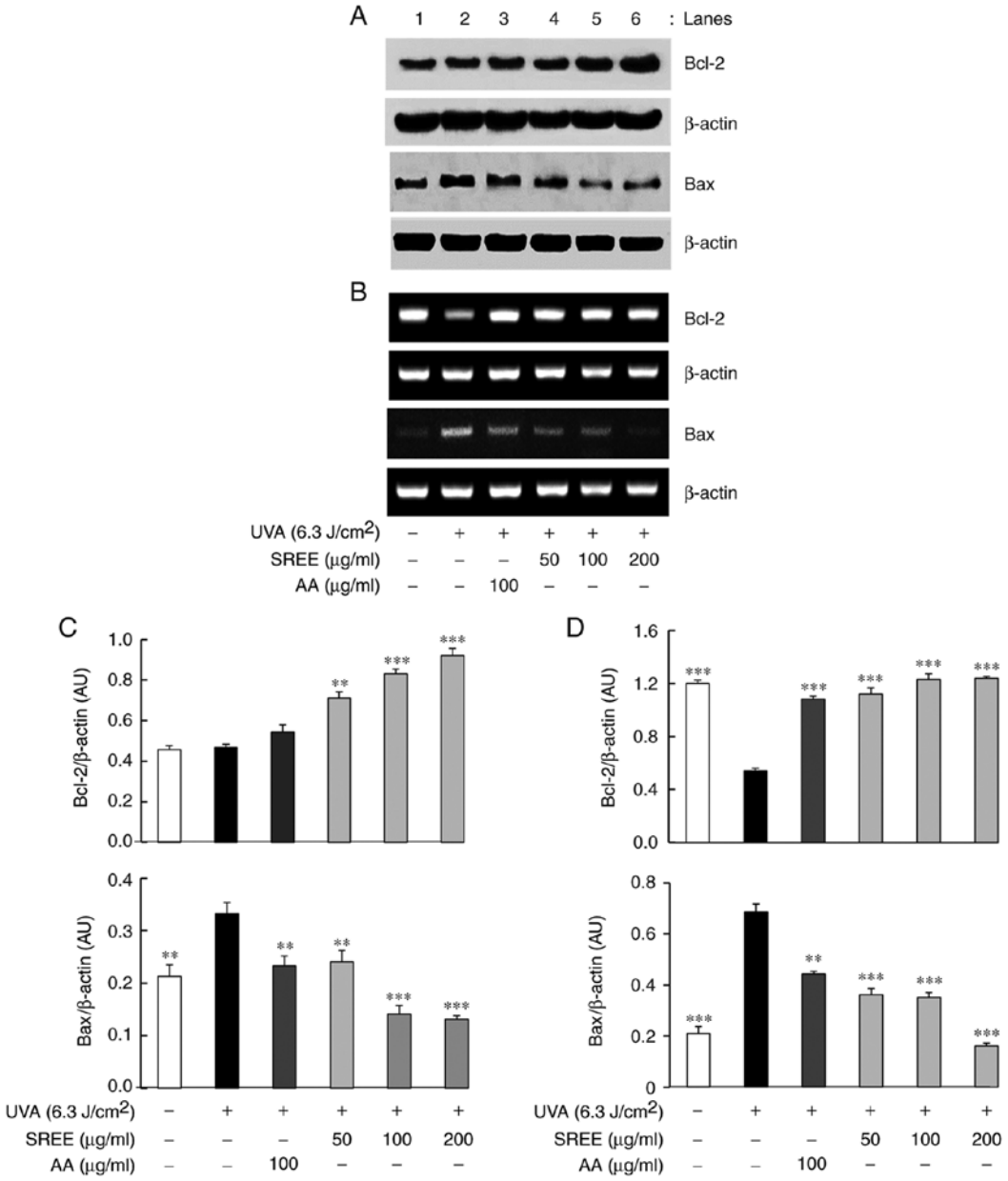

Figure 4. Effect of SREE on protein and mRNA expressions of Bcl-2 and Bax in UVA-irradiated human dermal fibroblasts. (A) Bcl-2 protein levels increased upon 24 h treatment with SREE in a dose-dependent manner compared to UVA-irradiated HDFs. Bax protein levels decreased upon 24 h treatment with SREE in a dose-dependent manner compared to UVA-irradiated cells. (B) Bcl-2 mRNA transcript levels increased upon 24 h treatment with SREE in a dose-dependent manner compared to UVA-irradiated cells. Bax mRNA transcript levels decreased upon 24 h treatment with SREE in a dose-dependent manner compared to UVA-irradiated cells. (C) Quantification of protein expression levels of Bcl-2 or Bax normalized to those of β-actin in (A). (D) Quantification of mRNA expression levels of Bcl-2 or Bax normalized to those of β-actin in (B). Values are presented the mean ± standard deviation of three independent experiments. **P<0.01, ***P<0.001 vs. control (UVA only). SREE, *Stachys riederi* var. *japonica* ethanol extract; AA, ascorbic acid; UVA, ultraviolet A; HDFs, human dermal fibroblasts; Bcl-2, B cell lymphoma 2; Bax, Bcl-2-associated X protein.

and *in vivo* (10,27). Conversely, an additional member of the Bcl-2 family Bax, usually identified in the cytosol, is a pro-apoptotic protein that perturbs the barrier function of mitochondrial membrane and induces apoptosis, primarily by translocating from the cytosol to the outer membrane of mitochondria (28). There is additionally evidence that Bax serves as a sentinel for cellular damage, as cytotoxic signals induce Bax translocation to the outer membrane of mitochondria, where it promotes mitochondrial dysfunction and triggers apoptosis (28,29). Notably, the present study demonstrated that SREE markedly interfered with the ability of UVA to downregulate mRNA and protein expressions of Bcl-2 in HDFs; however, it was additionally demonstrated that markedly attenuated UVA-induced increases in Bax expression at the mRNA and protein expression levels in the cells. These results suggest that SREE exhibited a protective effect on the mitochondrial membrane integrity in UVA-irradiated HDFs through regulation of the expression of Bcl-2 and Bax, and that the SREE-induced up- and downregulation of Bcl-2 and Bax expression in these cells occurs at the transcriptional level.

The opening of mitochondrial permeability transition pore is closely associated with increased permeability and loss of the $\Delta\Psi$m (30). Previously, ROS-induced depolarization of

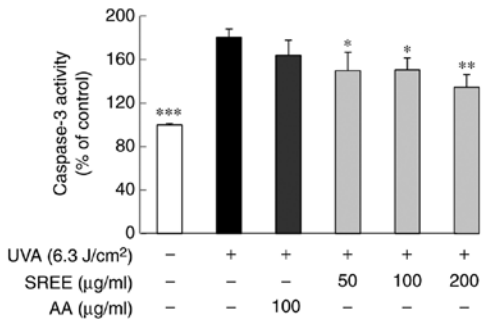

Figure 5. Effect of SREE on caspase-3 activity in UVA-irradiated HDFs. HDFs were exposed to UVA and grown in the absence or presence of SREE or AA at the indicated concentrations for 24 h. Whole cell lysates from the conditioned cells were prepared, and activity of caspase-3 was determined by using colorimetric caspase-3 assay kit. Values are presented as the mean ± standard deviation of three independent experiments. *P<0.05, **P<0.01, ***P<0.001 vs. control (UVA only). SREE, *Stachys riederi* var. *japonica* ethanol extract; AA, ascorbic acid; HDFs, human dermal fibroblasts.

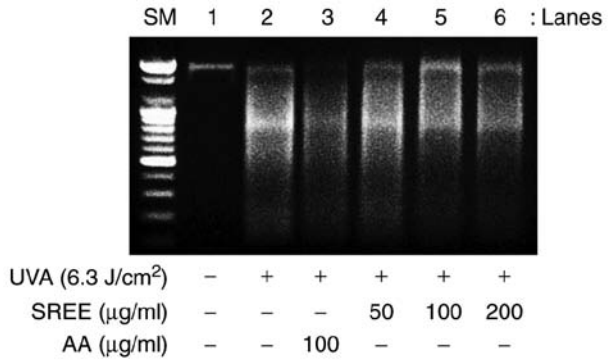

Figure 6. Effect of SREE on UVA-induced DNA fragmentation in HDFs. HDFs were exposed to UVA and grown in the absence or presence of SREE or AA at the indicated concentrations for 24 h. Genomic DNA from the conditioned cells were isolated and resolved on a 1% agarose gel. Fragmented DNA was visualized by ethidium bromide staining under ultraviolet light. SREE, *Stachys riederi* var. *japonica* ethanol extract; AA, ascorbic acid; HDFs, human dermal fibroblasts; SM, DNA size marker.

the ΔΨm and cytochrome *c* release from the mitochondria to the cytosol have been proposed (31). The present study demonstrated the ability of SREE to significantly inhibit UVA-induced loss of the ΔΨm in HDFs. These data suggested that SREE may have the ability to prevent depolarization of the ΔΨm and to inhibit release of cytochrome *c* from the mitochondria to the cytosol in UVA-irradiated HDFs, which is in part attributable to the antioxidant properties of SREE. Cytochrome *c* is a well-characterized mobile electron transport protein that is essential to energy conversion in all aerobic organisms. However, in cells undergoing apoptosis, high levels of cytochrome *c* are released from the mitochondrial membrane to the cytosol, where they subsequently trigger activation of the caspase family members (32,33). Among those, caspases-3 is at the core of the execution phase of apoptosis and its activation is regarded as one of the biochemical hallmarks of apoptosis (7). Accumulating evidence additionally indicates that cells undergoing apoptosis are characterized by nuclear DNA fragmentation (28,34). As SREE markedly suppressed the activation of caspase-3 and DNA fragmentation induced by UVA in HDFs, it was hypothesized that SREE exerted its cytoprotective effect on UVA-irradiated HDFs by inhibiting caspase-3 and apoptosis.

In conclusion, to the best of our knowledge, the present study is the first to indicate that SREE exhibited antioxidant and cytoprotective effects on UVA-irradiated human dermal fibroblasts, which may be mediated through the suppression of ROS generation, inhibition of the loss of the ΔΨm, Bcl-2 upregulation and Bax downregulation, caspase-3 inactivation and inhibition of apoptosis.

Acknowledgements

Not applicable.

Funding

No funding was received.

Availability of data and materials

All data generated or analyzed during this study are included in this published article.

Authors' contributions

JYH and AKY performed experiments. BCJ and YCK analysed the data and wrote the manuscript. All authors read and approved the final manuscript.

Ethics approval and consent to participate

Not applicable.

Patient consent for publication

Not applicable.

Competing interests

The authors declare that they have no competing interests.

References

1. Sarasin A: The molecular pathways of ultraviolet-induced carcinogenesis. Mutat Res 428: 5-10, 1999.
2. Wondrak GT, Roberts MJ, Cervantes-Laurean D, Jacobson MK and Jacobson EL: Proteins of the extracellular matrix are sensitizers of photo-oxidative stress in human skin cells. J Invest Dermatol 121: 578-586, 2003.
3. Jin GH, Liu Y, Jin SZ, Liu XD and Liu SZ: UVB induced oxidative stress in human keratinocytes and protective effect of antioxidant agents. Radiat Environ Biophys 46: 61-68, 2007.
4. Pavey S, Russell T and Gabrielli B: G2 phase cell cycle arrest in human skin following UV irradiation. Oncogene 20: 6103-6110, 2001.
5. Sung LY and Sung KL: Ultraviolet radiation: DNA damage, repair, and human disorders. Mol Cell Toxicol 13: 21-28, 2017.
6. Sheikh MS, Antinore MJ, Huang Y and Fornace AJ Jr: Ultraviolet-irradiation-induced apoptosis is mediated via ligand independent activation of tumor necrosis factor receptor 1. Oncogene 17: 2555-2563, 1998.
7. Savitskaya MA and Onishchenko GE: Mechanisms of apoptosis. Biochemistry (Mosc) 80: 1393-1405, 2015.
8. He B, Lu N and Zhou Z: Cellular and nuclear degradation during apoptosis. Curr Opin Cell Biol 21: 900-912, 2009.

9. Sitailo LA, Tibudan SS and Denning MF: Activation of caspase-9 is required for UV-induced apoptosis of human keratinocytes. J Biol Chem 277: 19346-19352, 2002.
10. Assefa Z, Garmyn M, Vantieghem A, Declercq W, Vandenabeele P, Vandenheede JR and Agostinis P: Ultraviolet B radiation-induced apoptosis in human keratinocytes: Cytosolic activation of procaspase-8 and the role of Bcl-2. FEBS Lett 540: 125-132, 2003.
11. Salucci S, Burattini S, Battistelli M, Baldassarri V, Maltarello MC and Falcieri E: Ultraviolet B (UVB) irradiation-induced apoptosis in various cell lineages in vitro. Int J Mol Sci 14: 532-546, 2012.
12. Lei L, Li H and Zhen-Zhen Z: Activation of JNK/Bim/Bax pathway in UV-induced apoptosis. Proc SPIE 7900, Biophotonics Immune Responses VI; 79000I, 79000I, 2011.
13. Assefa Z, Van Laethem A, Garmyn M and Agostinis P: Ultraviolet radiation-induced apoptosis in keratinocytes: On the role of cytosolic factors. Biochim Biophys Acta 755: 90-106, 2005.
14. Green DR and Reed JC: Mitochondria and apoptosis. Science 281: 1309-1312, 1998.
15. Liu X, Kim CN, Yang J, Jemmerson R and Wang X: Induction of apoptotic program in cell-free extracts: Requirement for dATP and cytochrome c. Cell 86: 147-157, 1996.
16. Tundis R, Peruzzi L and Menichini, F: Phytochemical and biological studies of Stachys species in relation to chemotaxonomy: A review. Phytochemistry 102: 7-39, 2014.
17. Sadeghi H, Zarezade V, Sadeghi H, AkbartabarToori M, Jafari Barmak M, Azizi A, Ghavamizadeh M and Mostafazadeh M: Anti-inflammatory activity of Stachys Pilifera Benth. Iran Red Crescent Med J 16: e19259, 2014.
18. Hajhashemi V, Ghannadi A and Sedighifar S: Analgesic and anti-inflammatory properties of the hydroalcoholic, polyphenolic and boiled extracts of Stachys lavandulifolia. Res Pharm Sci 1: 92-98, 2007.
19. Shin TY: Stachys riederi inhibits mast cell-mediated acute and chronic allergic reactions. Immunopharmacol Immunotoxicol 26: 621-630, 2004.
20. Denning MF, Wang Y, Tibudan S, Alkan S, Nickoloff BJ and Qin JZ: Caspase activation and disruption of mitochondrial membrane potential during UV radiation-induced apoptosis of human keratinocytes requires activation of protein kinase C. Cell Death Differ 9: 40-52, 2002.
21. Gorczyca W, Gong J and Darzynkiewicz Z: Detection of DNA strand breaks in individual apoptotic cells by the in situ terminal deoxynucleotidyl transferase and nick translation assays. Cancer Res 53: 1945-1951, 1993.
22. Phaniendra A, Jestadi DB and Periyasamy L: Free radicals: Properties, sources, targets, and their implication in various diseases. Indian J Clin Biochem 30: 11-26, 2015.
23. Genova ML, Pich MM, Bernacchia A, Bianchi C, Biondi A, Bovina C, Falasca AI, Formiggini G, Castelli GP and Lenaz G: The mitochondrial production of reactive oxygen species in relation to aging and pathology. Ann N Y Acad Sci 1011: 86-100, 2004.
24. Adams JM and Cory S: The BCL-2 arbiters of apoptosis and their growing role as cancer targets. Cell Death Differ 25: 27-36, 2018.
25. Borner C: The Bcl-2 protein family: Sensor and checkpoints for life-or-death decisions. Mol Immunol 39: 615-647, 2003.
26. Shamas-Din A, Kale J, Leber B and Andrews DW: Mechanisms of action of Bcl-2 family proteins. Cold Spring Harb Perspect Biol 5: a008714, 2013.
27. Takahashi H, Honma M, Ishida-Yamamoto A, Namikawa K, Miwa A, Okado H, Kiyama H and Iizuka H: In vitro and in vivo transfer of bcl-2 gene into keratinocytes suppresses UVB-induced apoptosis. Photochem Photobiol 74: 579-586, 2001.
28. Gross A, Jockel J, Wei MC and Korsmeyer SJ: Enforced dimerization of BAX results in its translocation, mitochondrial dysfunction and apoptosis. EMBO J 17: 3878-3885, 1998.
29. Banerjee G, Gupta N, Kapoor A and Raman G: UV induced by stander signaling leading to apoptosis. Cancer Lett 223: 275-284, 2005.
30. Bonora M and Pinton P: The mitochondrial permeability transition pore and cancer: Molecular mechanisms involved in cell death. Front Oncol 4: 302, 2014.
31. Gogvadze V, Orrenius S and Zhivotovsky B: Multiple pathways of cytochrome c release from mitochondria in apoptosis. Biochim Biophys Acta 1757: 639-647, 2006.
32. Orrenius S, Gogvadze V and Zhivotovsky B: Calcium and mitochondria in the regulation of cell death. Biochem Biophys Res Commun 460: 72-81, 2015.
33. Schuler M, Bossy-Wetzel E, Goldstein JC, Fitzgerald P and Green DR: p53 induces apoptosis by caspase activation through mitochondrial cytochrome c release. J Biol Chem 275: 7337-7342, 2000.
34. Kitazumi I and Tsukahara M: Regulation of DNA fragmentation: The role of caspases and phosphorylation. FEBS J 278: 427-441, 2011.